Behavior and design of fastenings with bonded anchors: numerical analysis and experimental verification

R. Eligehausen & J. Appl
Institute for Construction Materials, University of Stuttgart, Stuttgart, Germany

ABSTRACT: This paper presents the results of extensive numerical and experimental work performed to establish a behavioral model that provides the basis for developing design provisions for anchorages to concrete using adhesive bonded anchors. These types of anchorage systems are used extensively. The behavioral model is compared to a worldwide data base containing 415 tests on adhesive anchor groups, 133 tests on adhesive anchors located near a free edge.

1 INTRODUCTION

A wide spectrum of bonded anchor systems are currently available. A distinction can be made between so called capsule systems and injection systems. For both systems the bonding materials may consist of polymer resins, cementitious materials, or a combination of the two.

Capsule anchor systems employ a threaded rod equipped with a 45° chisel- or roof shaped tip and a hexagonal nut and washer. The glass capsule is filled with the constituent bonding materials. It contains polymer resin, hardener and quartz aggregate in a defined mix ratio.

For injection systems resin and hardener are contained in separate chambers.

The embedment depth of capsule systems can be 8 to 10 times of the diameter of the rod; for injection systems the embedment depth can be user defined, but it should not exceed the limit of 20 times the rod diameter. The capsule is placed in a hole from which all drilling dust has been removed. When driving the threaded rod into the hole, the glass capsule is broken and fragmented, the resin, hardener and aggregates and capsule fragments are mixed and the annular gap around the threaded rod is filled with the polymeric matrix.

For injection systems the injection of the components into the drilled hole is accomplished with the aid of a mechanical or pneumatic dispenser. Conventional bonded anchors are not ideal for resisting tension loads in concrete that is subjected to cracking. Therefore special bonded anchors for uncracked concrete have been developed, so called bonded undercut or bonded expansion anchors. More details

for the different anchoring systems are included in Eligehausen et al. (2006).

2 BACKGROUND

2.1 *Headed cast – in place and post- installed mechanical anchors*

Fuchs et al. (1995) proposed a behavioral model for concrete breakout failure. This model was created to predict the failure loads of cast-in-place headed anchors and post-installed mechanical anchors loaded in tension or in shear that exhibit concrete breakout failure. According to Fuchs et al. (1995), the mean concrete breakout capacity for single cast-in-place anchors and post-installed mechanical anchors in uncracked concrete unaffected by edge influences or overlapping cones of neighboring anchors loaded in tension is given by the following equations:

Cast-in-place anchors:

$$N_{u,c}^{0} = 15.5 \cdot f_{cc}^{0.5} \cdot h_{ef}^{1.5} \qquad (N) \qquad (1a)$$

Post-installed mechanical anchors:

$$N_{u,c}^{0} = 13.5 \cdot f_{cc}^{0.5} \cdot h_{ef}^{1.5} \qquad (N) \qquad (1b)$$

where f_{cc} = concrete compressive strength measured on cubes with a side length of 200mm; and h_{ef} = embedment depth.

If fastenings are located so close to an edge that there is not enough space for a complete concrete cone to develop, the load-bearing capacity of the anchorage is also reduced. For anchor groups with a spacing smaller than a critical value it is found, that

the failure load is reduced with decreasing spacing, which is called group effect. The critical value is called characteristic spacing $s_{cr,N}$. The concrete breakout capacity of anchor groups $N_{u,c}$ and anchors located near free edges with a tension load applied concentrically to the anchors is given by Equation 2 where $N_{u,c}^0$ is taken from Equation 1:

$$N_{u,c} = N_{u,c}^0 \cdot \frac{A_{c,N}}{A_{c,N}^0} \cdot \psi_{s,N} \qquad \text{(N)} \qquad (2)$$

with

$$\psi_{s,N} = 0.7 + 0.3 \cdot \frac{c}{c_{cr,N}} \leq 1.0 \quad \text{(-)} \qquad (2b)$$

where c = edge distance; $c_{cr,N}$ = characteristic distance; $\psi_{s,N}$ = factor to consider disturbance of radial symmetric stress distribution caused by an edge; $A_{c,N}^0$ = projected area of one anchor at the concrete surface unlimited by edge influences or neighboring anchors, idealizing the failure cone as a pyramid with the base length $s_{cr,N}$; and $A_{c,N}$ = actual projected area at the concrete surface, assuming the failure surface of the individual anchors as a pyramid with a base length $s_{cr,N}$. Figure 1 provides information on how projected areas $A_{c,N}^0$ and $A_{c,N}$ are determined. According to Fuchs et al. (1995), for cast-in-place and post-installed mechanical anchors, the characteristic spacing, $s_{cr,N}$, is $3.0h_{ef}$ and the characteristic edge distance, $c_{cr,N}$, is $1.5\,h_{ef}$.

One of the principal advantages of this model is that calculation of the changes in capacity due to factors such as edge distance, spacing, geometric arrangement of groupings, and similar variations can be readily determined though use of relatively simple geometrical relationships based on rectangular prisms.
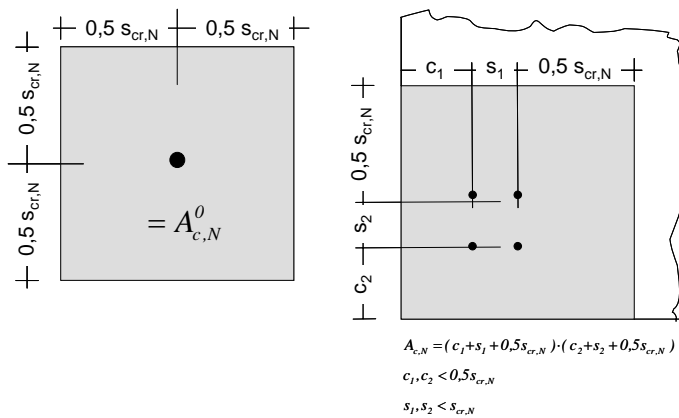
(a)   (b)

Figure 1. Calculation of effective areas: (a) single anchors away from edges and anchors; and (b) groups of 4 closely spaced anchors located near a corner

2.2 Single bonded anchors

Bonded anchors resist tension load by adhesion and micro-keying of the resin and by mechanical interlock to the anchors rod to the sides of the drilled

hole and by mechanical interlock to the anchor rod. The tension forces are transferred to the surrounding concrete by radially symmetric compression struts that spread out from the anchor. This in turn generates tension stresses perpendicular to the compression struts. Due to the load-transfer mechanism and available bond strength different failure modes can be observed. Figure 2 shows typical failure modes of single bonded anchors. If bond strength is high enough to utilize the tension strength of the concrete, concrete failure will occur which is characterized by cone-shaped concrete breakout originating at the base of the anchor (Fig. 2a). The slope of the cone envelope with the respect to the surface of the concrete member is approximately 25° to 35°. Normally, this failure mode can be observed at small embedment depth ($h_{ef} \sim 3d$-$5d$). For greater embedment depth the failure mode shifts from a concrete cone to a mixed mode type of failure. A concrete cone with a depth of approximately $2d$ to $3d$ forms at the top end of the anchor and bond failure occurs along the remaining length of the anchor. Bond failure occurs either at the boundary between threaded rod and mortar (Interface 1, Fig. 2c) or between the mortar and the sides of the drilled hole (Interface 2, Fig. 2b). Often a mixed interface failure can be observed (Fig. 2d). For large embedment depths steel failure can occur.
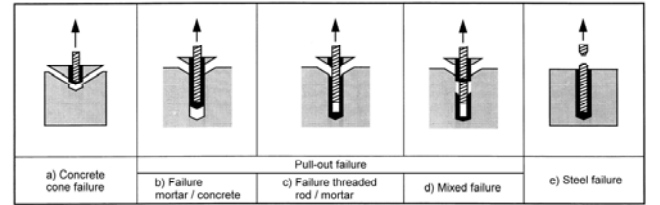

Figure 2. Possible embedment-related failure modes of bonded anchors (Cook et al. 1998).

Experimental studies discussed in Eligehausen et al. (2004), indicate that the actual bond stress distribution along the embedment length at peak load is nonlinear with lower bond stresses at the concrete surface and higher bond stresses at the embedded end of the anchor. However, in Cook et al. (1998) a comparison of suggested behavioral models with a worldwide data base for single adhesive anchors indicates that their failure load is best described by a uniform bond stress model incorporating the nominal anchor diameter (d) with the mean bond stress ($\tau_{u,m}$) associated with each product. This is confirmed by experimental and numerical studies of Meszaros (1999) and McVay et al. (1996). The uniform bond stress model for adhesive anchors is given by Equation 3. This equation is valid for $4 \leq h_{ef}/d \leq 20$.

$$N^0_{u,m,p} = \pi \cdot d \cdot h_{ef} \cdot \tau_{u,m} \quad \text{(N)} \qquad (3)$$

where $N^0_{u,m,p}$ = average failure load of single bonded anchor failing by pullout (Fig. 2); d = diameter of the anchor rod; h_{ef} = embedment depth; and $\tau_{u,m}$ = average bond strength.

Assuming that the maximum failure load of bonded anchors is limited to the concrete breakout failure load of post-installed mechanical anchors as given by Equation 1 the upper limit of the bond strength to be used for single anchors can be determined by equating Equation 1 with Equation 3:

$$\tau_{u,max} = 4.2 \cdot \frac{f_{cc}^{0,5} \cdot h_{ef}^{0,5}}{d} \quad \text{(N/mm²)} \qquad (4)$$

3 NUMERICAL ANALYSIS AND EXPERIMENTAL TESTS OF ADHESIVE ANCHORS

3.1 Microplane model

In the following numerical study, the finite element code MASA which is based on the microplane model, was used. MASA was developed for two-and three-dimensional analysis of quasi-brittle materials. In the model the material is characterized by a uniaxial relation between the stress and strain components of planes of various orientations. At each integration point these planes may be imagined to represent the damage planes or weak planes of the microstructure (Fig. 3). Tensorial invariance restrictions need to be directly enforced. Superimposing the response from all microplanes in a suitable manner automatically satisfied them. The model allows for a realistic prediction of the material behavior in case of three-dimensional stress-strain states. A smeared crack approach is employed. To ensure mesh independent results the crack band approach is used. More details about the model can be found in Ozbolt (1998).
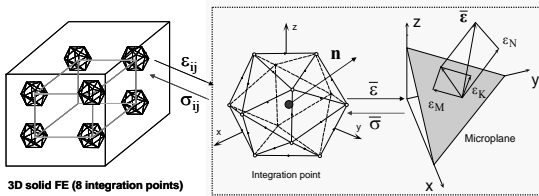

(a)   (b)

Figure 3. Concept of microplane model: (a) Integration points; and (b) unit volume sphere and strain components (Ozbolt 1998).

3.2 Modelling

3.2.1 General

To understand the behavior of adhesive anchors under tension loading, three-dimensional non-linear fi-nite element analyses were performed. The mortar behavior was simulated using the microplane model with a proper calibration of the model parameters to represent the measured macroscopic mortar properties. The load transfer between threaded rod and mortar results from mechanical interlock between thread and mortar consoles. In this case the maximum load that can be transferred at the interface is mainly influenced by the macroscopic properties of the mortar. On the contrary, the maximum load which can be transferred between mortar and concrete is mainly influenced by the microscopic properties of the mortar and the concrete. However, the material's behavior of the interface mortar/concrete can hardly be described by means of theoretical model. At the moment there is no all-purpose adhesion theory. Main influencing parameters on the adhesion are bonding forces, ratio of adhesion and cohesion, polarity, porosity and roughness of the adjacent materials. Consequently the complicated process of penetration and curing of the mortar in the concrete must be taken into account by special contact-elements which are located between mortar and concrete elements. Figure 4 shows the stress-strain relationships of macroscopic mortar elements for three different mortar types which depend on the polymeric resins and the fillers used.
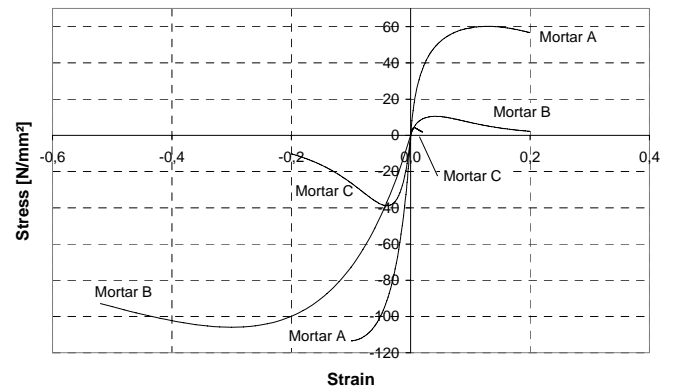

Figure 4. Macroscopic stress-strain relationship of mortar elements.

Simulated were single adhesive anchors near to and far away from an edge, as well as quadruple anchor groups with four and six bonded anchors. Parameters varied for single anchors were anchor diameter, embedment depth, bond strength of the mortar, concrete compressive strength and edge distance. For anchor groups the spacing of the anchors was also varied. In all numerical simulations, the member thickness was large enough to avoid splitting failures. The loading process was displacement-controlled, by applying incremental displacements to the anchor at the concrete surface.

3.2.2 *Single bonded anchors*

The geometry of the specimen and the finite element mesh are shown in Figure 5. A concrete slab with a width of $6h_{ef}$ and a height of $3h_{ef}$ is analysed. The materials properties of the concrete are equal to the properties measured in experiments. The existing symmetry planes were used to reduce the analysis time. The mesh was refined within the area of the bonded anchor. The modeled test specimen is re-strained in vertical direction at a distance of $3h_{ef}$ from the anchor. The numerical analysis considers the same boundary conditions as in experiments with unconfined tests. The anchor was discretized by three-dimensional linear elastic finite elements.
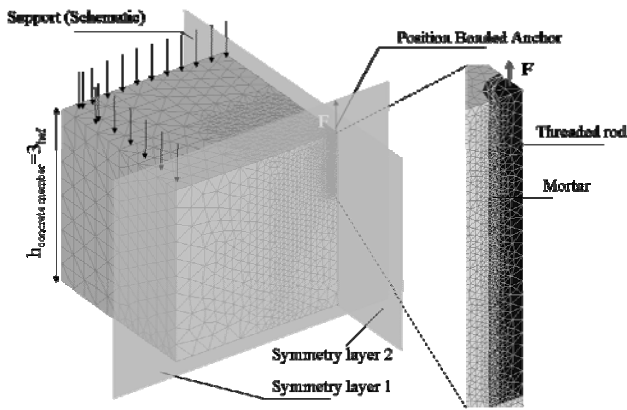
Figure 5. Typical FE meshes of concrete block and adhesive anchor.

Figure 6 shows the modeled threaded rod and the mortar layers. The geometry of the thread was sim-plified compared to a real threaded rod. The mod-eled thread runs perpendicular to the shaft.
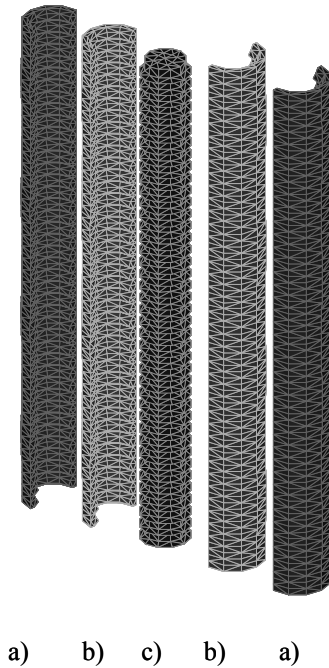

a)   b)   c) b)   a)

Figure 6. Typical FE meshes of an adhesive anchor:
(a) Mortar elements (microscopic properties); (b) Mortar elements (macroscopic properties); and (c) Steel elements.

3.2.3 *Groups with bonded anchors*

The geometry of the specimen for anchor groups and the finite element mesh are shown in Figure 7. The geometry is similar to that for single anchors. Only a slab with a width of $6h_{ef}+s$ and a thickness of $3h_{ef}$ is analysed. The parameters under investigation in-cluded anchor diameter, embedment depth, concrete strength, bond strength and anchor spacing.
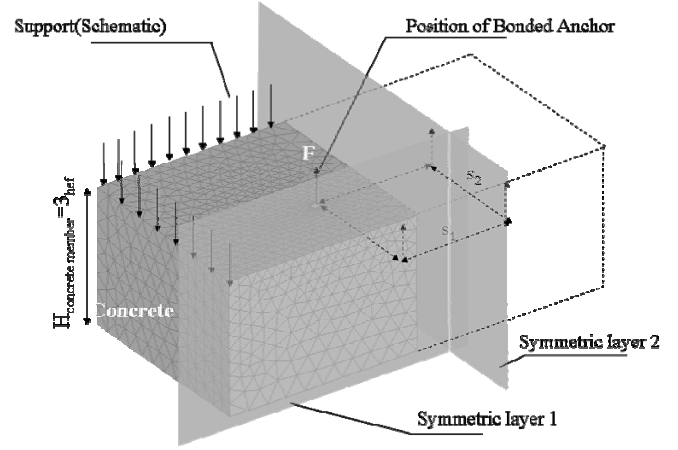

Figure 7. Typical FE mesh of concrete block for a group of adhesive anchors.

3.3 *Pullout failure*

3.3.1 *Single bonded anchors*

Figure 8 show the numerical results concerning the principal strains in the concrete after the peak load, for a single bonded anchor wit a bond strength of $\tau_{u,m} = 9.3$ N/mm² and diameter of d = 24mm, as well as a photograph of the anchor after tension test. Dark areas in Figure 8a characterize crack formation. With a embedment depth of $10d$ just to the peak load a shallow cone is formed at the concrete surface and bond failure occurs along the remaining length of the anchor.
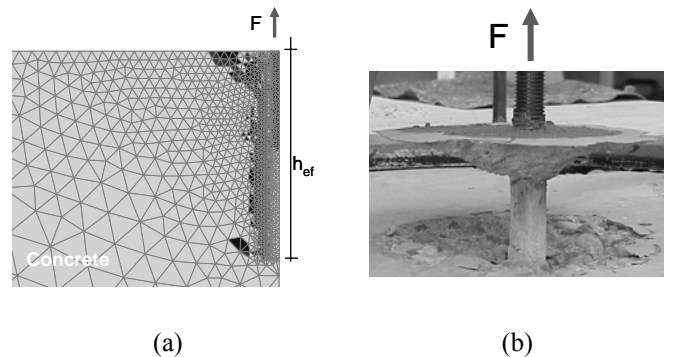

(a)   (b)

Figure 8. Failure mode of bonded anchor: (a) Numerical re-sult; and (b) Test result

3.3.2 *Groups with bonded anchors*

Figure 9 shows the principal tensile strains for a group of four bonded anchors with $d = 12$mm, $h_{ef} = 10d$, and $\tau_{u,m} = 9.3$ N/mm² after passing peak load.

With a small spacing of $s = 4d$, a common concrete cone breakout cone starting at the base of the anchors is formed (Fig. 9a). With a larger spacing ($s=16d$), the individual anchors of the group fail in the same way as single anchors with a pullout failure similar to that shown in Figure 8. The failure load of anchorages with adhesive anchors can be calculated by means of Equation 2 that needs to be modified with reference to bond strength, anchor spacing and anchor distance from a nearby edge.
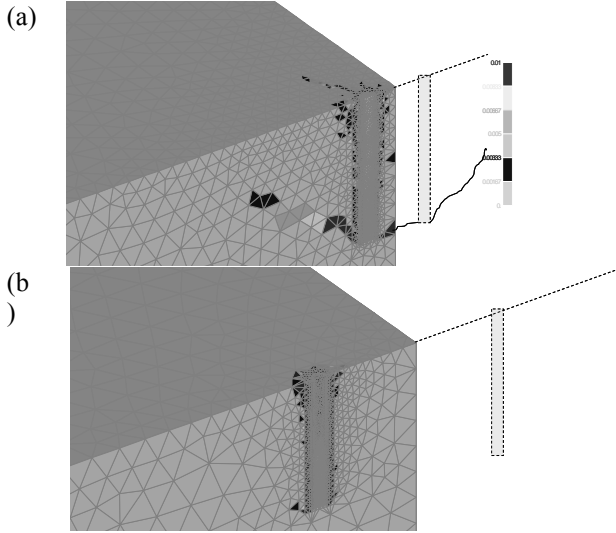
(a)

(b)

Figure 9. Failure modes of quadruple anchor group with bonded anchors ($d = 12$mm, $h_{ef} = 10$d, $\tau_{u,m} = 9.3$ N/mm²): (a) $s = 4d$; and (b) $s = 16 d$.

As indicated by Equation 3, the average bond strength ($\tau_{u,m}$), the anchor diameter (d), and the anchor embedment length (h_{ef}) represent the parameters that influence the characteristic spacing and the characteristic edge distance.
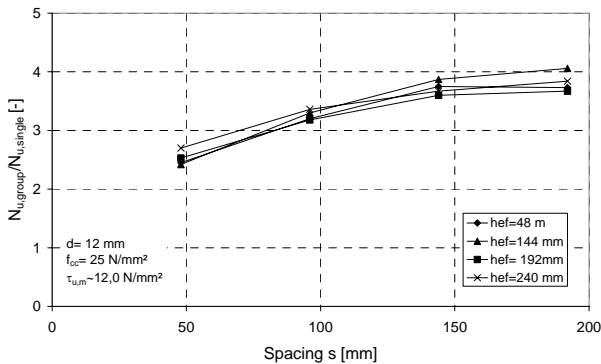
Figure 10. Numerically-obtained failure load of quadruple groups in case of pullout failure related to the failure load of a single anchor as a function of the spacing (Li et al. 2002).

As a result of the numerical studies by Li et al. (2002), it was determined that the characteristic spacing is not significantly influenced by the embedment depth (h_{ef}) of the anchors. This is shown in Figure 10 where the ratios between the numerically

obtained failure loads of groups with bonded anchors to the failure load of single anchors with the same embedment depth are plotted as a function of the anchor spacing, for different values of embedment depth h_{ef}.
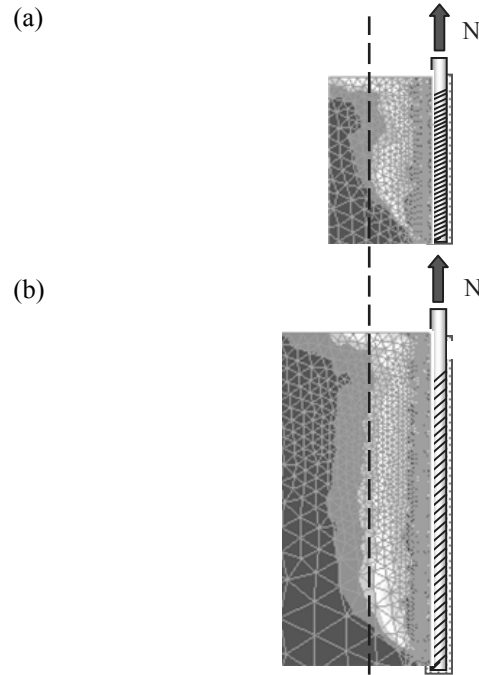
(a)

(b)

Figure 11. Principal compression stresses in concrete. Single adhesive anchors: (a) $d = 12$mm, $h_{ef}/d = 10$; and (b) $d =12$mm, $h_{ef}/d = 20$.

If the characteristic spacing were influenced by the embedment depth, groups with a smaller embedment depth would reach the capacity of four single anchors at a smaller spacing than those with a larger embedment depth. However, for a given spacing, the related failure load is hardly dependent on the embedment depth. This behavior is explained by Figure 11 where - in the case of pullout failure - the width of the principal compression stress field of single bonded anchors with constant bond strength and significantly different embedment lengths is nearly identical. The width of the compression stress field is directly related to the characteristic spacing.
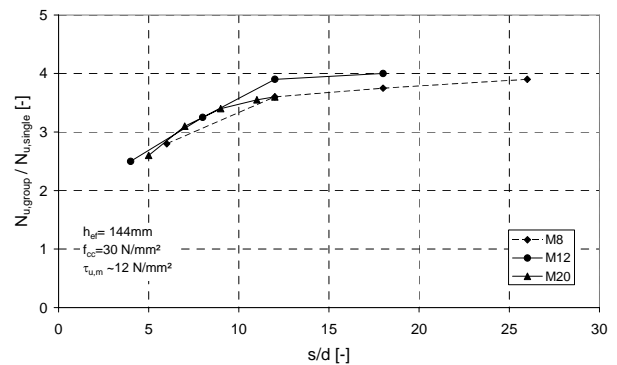
Figure 12. Numerically-obtained failure load of quadruple groups in case of pullout failure related to the failure load of a single anchor as a function of the related spacing (Li et al. 2002).

Li et al. (2002) found that the characteristic spacing is dependent on anchor diameter (d). This can be seen in Figure 12 that shows related failure loads of groups of anchors with different diameters as a function of the related spacing (s/d).

The related group failure load is almost independent of the anchor diameter for a constant ratio of s/d and reaches the full capacity of four individual anchors at about the same value of s/d.

Studies by Li et al. (2002) indicated that the characteristic spacing is also influenced by the average bond strength $\tau_{u,m}$.
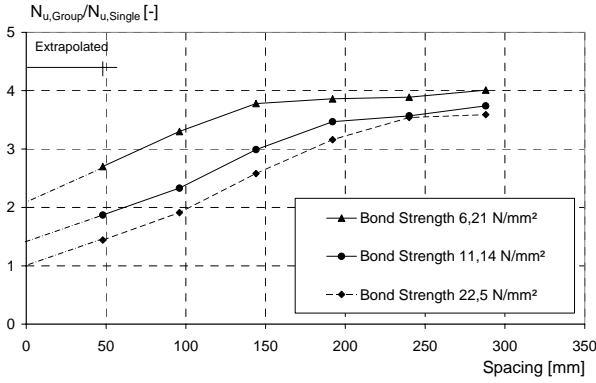

Figure 13. Numerically-obtained failure load of quadruple groups in case of pullout failure related to the failure load of a single anchor as a function of the spacing.
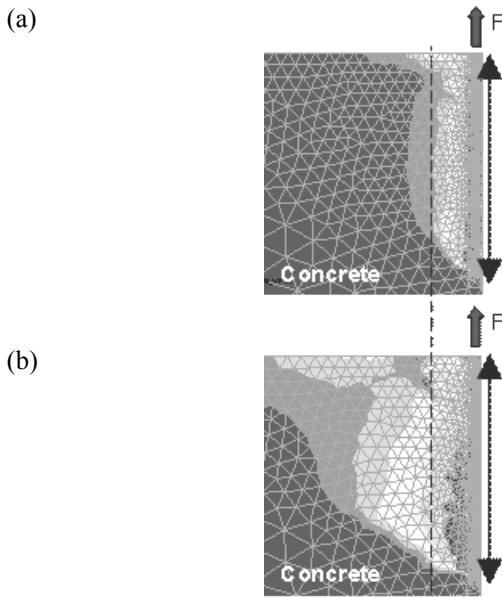
(a)

(b)

Figure 14. Principal compression stresses in concrete. Single adhesive anchors ($d = 24$, $h_{ef}/d = 20$): (a) $\tau_{u,m} = 9.9$ N/mm²; and (b) $\tau_{u,m} = 19.6$ N/mm².

In Figure 13, the ratio of the anchor group strength to the single anchor strength is plotted as a function of anchor spacing. According to the analysis, the anchor diameter and embedment depth were kept constant and bond strength was varied. For anchorages with the highest bond strength, failure occurred by concrete breakout. Therefore the assumed bond strength was not fully utilized. The characteristic spacing obtained in the analysis is about 300mm:

For the minimum embedment depth $h_{ef} = 96$mm the characteristic spacing is about $s_{cr,Np} = 3h_{ef}$. With decreasing bond strength the characteristic spacing decreases. The assumption that the characteristic spacing is influenced by the bond strength is confirmed by Figure 14 which shows that the width of the principal compression stress field of a single anchor with constant embedment depth increases with increasing bond strength.

To determine the characteristic spacing, ($s_{cr,Np}$) for each individual numerical test series, the ratios $N_{u,group}/N_{u,single} = f_{(scr,N)}$ were approximated by an exponential function which was found by regression analysis (Fig. 15).
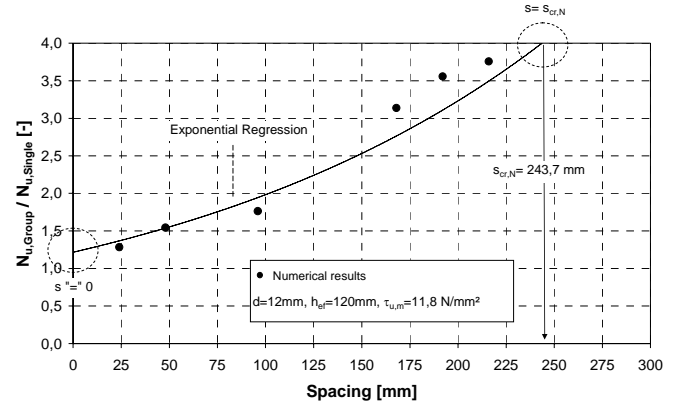

Figure 15. Numerically-obtained failure loads of quadruple groups in related to the failure load of a single anchor as a function of spacing.

The characteristic spacing was determined by extrapolating this function to the value of $N_{u,group}/N_{u,single} = 4$. Figure 16 provides a summary of the results. The values of the characteristic spacing found from each test series divided by the diameter ($s_{cr,Np}/d$) are plotted as a function of bond strength. For comparison the characteristic spacing evaluated in the same way from results of tests are shown as well.
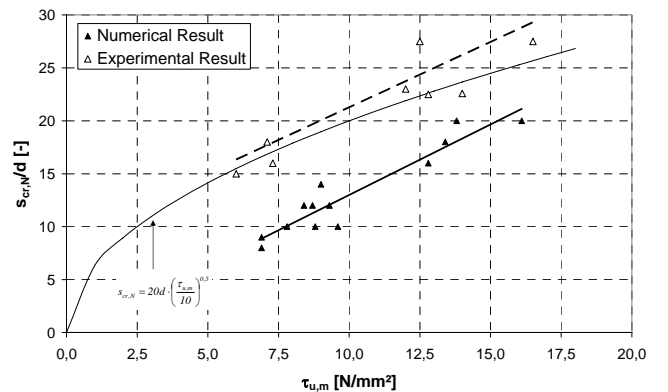

Figure 16. Related critical spacing $s_{cr,N}/d$ as a function of mean bond strength.

It is obvious that the characteristic spacing found by numerical analysis is smaller than that evaluated by means of experimental tests. This is due to the fact,

that the numerical analysis does not take into account the stiffness of the plate and the scattering of the load-displacement curves of the single bonded anchors of a group. Based on the test results, the characteristic spacing can be approximated by Equation 5.

$$s_{cr,Np} = 20 \cdot d \cdot \left(\frac{\tau_{u,m}}{10}\right)^{0.5} \text{ (mm)} \qquad (5)$$

The characteristic edge distance ($c_{cr,Np}$) may be taken as one half of the characteristic spacing.

Based on the above considerations the failure load of adhesive anchor groups and/or anchorages located near edges can be calculated by Equation 2 with $N_{u,c}^0$ replaced by $N_{u,m,p}^0$ from Equation 3 and using $s_{cr,Np}$ and $c_{cr,Np}$ determined from Equation 5.

3.3.3 Concrete cone and pullout failure

In the case of concrete cone failure, the failure load of a group of anchors with a theoretical spacing $s = 0$ is equal to the value valid for a single anchor (Eqn. 2). However in case of combined concrete cone and pullout failure when extrapolating the regression lines that describe the failure loads of bonded anchor, the group failure load for a theoretical spacing of $s = 0$ is larger than that of a single anchor (Figs. 10,12,13,15). This increase is denoted by the factor $\psi_{g,N}^0$ in Figure 18. It is explained in Figure 17. If the bond strength is low the failure of two adjacent anchors is caused by bond failure resulting in anchor pullout. The bond failure area of the two adjacent anchors is approximately equal to $\sqrt{2}$ times the effective bond area of a single anchor and for a group of n anchors approximately $\sqrt{n}$ times the bond area of a single anchor. Therefore, the failure load of the group is $\sqrt{n}$ times the failure load of a single anchor ($\psi_{g,N}^0 = \sqrt{n}$). On the contrary, the failure load of a group of adjacent anchors is not increased over that of a single anchor when failure is controlled by concrete breakout ($\psi_{g,N}^0 = 1$). The value of $\psi_{g,N}^0$ should be related to the bond strength. If the bond strength is equal to $\tau_{u,max}$ according to Equation 4 then a single anchor will fail by concrete breakout and $\psi_{g,N}^0 = 1.0$. If the bond strength is very small (e.g. $\tau < 0.3$ $\tau_{u,max}$) then failure of the group will be caused by anchor pullout resulting in $\psi_{g,N}^0 \approx \sqrt{n}$. Values for $\psi_{g,N}^0$ between these limiting cases were determined from the results of the individual numerical test series of quadruple anchor groups. They are plotted in Figure 18 as a function of the ratio $\tau_u/\tau_{u,max}$ and can be approximated by Equation 6.

$$\psi_{g,N}^0 = \sqrt{n} \cdot \left(\sqrt{n} - 1\right)\left(\frac{\tau_{u,m}}{\tau_{u,max}}\right)^{1,5} \geq 1.0 \qquad (6)$$
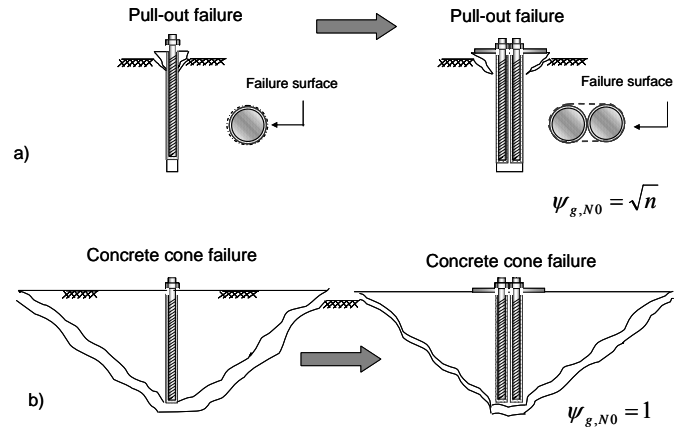

Figure 17. Increase of failure area and failure load: (a) pull-out failure; and (b) concrete cone failure.
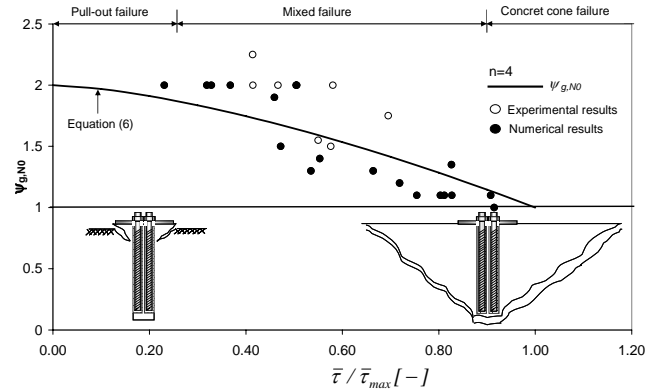

Figure 18. Factor $\psi_{g,N}^0$ as a function of mean bond strength $\tau_{u,m}$ related to the maximum value $\tau_{u,max}$ according to Equation 4.

Increasing the spacing among the anchors diminishes the favorable effects that a larger bonded area has on the failure load. This effect is taken into account by the factor $\psi_{g,N}$. It is assumed that this factor potentially decreases between $s = 0$ where $\psi_{g,N} = \psi_{g,N}^0$ and $s = s_{cr,Np}$ where $\psi_{g,N} = 1.0$. This leads to Equation 7.

$$\psi_{g,N} = \psi_{g,N}^0 - \left(\frac{s}{s_{cr,Np}}\right)^{0,5} \left(\psi_{g,N}^0 - 1\right) \qquad (7)$$

On the basis of the afore-mentioned considerations, the mean failure load of anchorages using adhesive anchors in case of pullout or combined concrete pullout failure may be calculated as follows:

$$N_{u,m,p} = N_{u,m,p}^0 \cdot \frac{A_{p,N}}{A_{p,N}^0} \cdot \psi_{s,N} \cdot \psi_{g,N} \qquad (8)$$

In Equation 8, $A_{p,N}$ and $A_{p,N}^0$ are determined according to Figure 1, $\psi_{s,N}$ is given by Equation 2b, $\psi_{g,N}$ is given by Equation 7, and $N_{u,m,p}^0$ is determined from Equation 3. The characteristic spacing $s_{cr,Np}$ and characteristic edge distance $c_{cr,Np}$ provided by Equation 5 should be used when calculating $A_{p,N}$ and $A_{p,N}^0$, $\psi_{s,N}$ and $\psi_{g,N}$.

3.4 Concrete cone failure

3.4.1 Single bonded anchors

Figure 19 and Figure 20 show the numerically obtained principal strains in the concrete after reaching the peak load for single anchors with a diameter $d = 6$mm, $d = 24$mm and a bond strength which is high enough to utilize the concrete cone strength. Figures 19a and 19b are valid for an anchor with $h_{ef}/d = 5$, while Figure 20 is valid for $h_{ef}/d = 10$. Dark areas in these figures characterize crack formation.
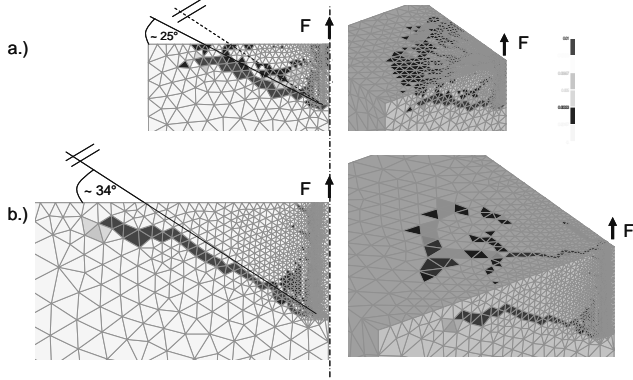

Figure 19. Concrete cone failure indicated by numerical modeling: (a) d= 6mm, h_{ef}/d=5; and (b) d= 24mm, h_{ef}/d= 5.

Similar to the experiments with an embedment length of $5d$ a crack forms at the base which grows with increasing imposed displacement resulting in a concrete breakout failure. The average angle of crack propagation in respect to the surface increases with increasing embedment depth from about 25° (h_{ef}= 30mm) to about 35° (h_{ef} = 120mm). This increase of the angle can be explained by fracture mechanics. Based on fracture mechanics, tension loaded anchors can be classified as a mixed-mode problem. With increasing crack length the ratio of the stress intensity factor for Mode 1 and for Mode 2 is changes. As a result, the mean value of the angle changes as well.
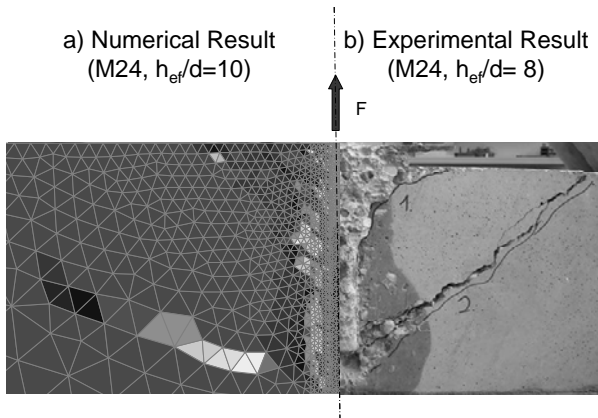

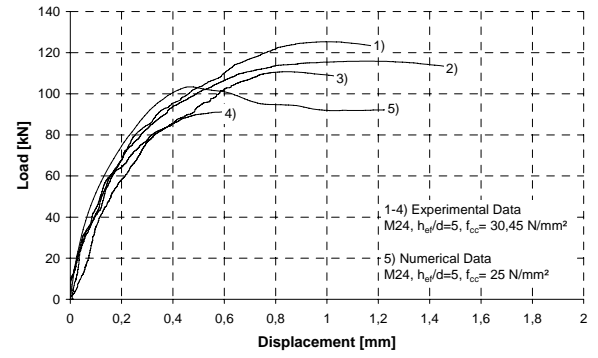Figure 20. Concrete cone failure predicted by numerical modeling and comparison with test result.

Figure 21. Numerically-obtained load-displacement curve in comparison to test result.

For a related embedment depth of $h_{ef}/d = 10$ similar as in experiment two internal cracks are formed. Failure is caused by the crack starting at the bottom of the anchor.

Figure 21 shows a comparison between load displacement curves measured in experiments and obtained numerically. The agreement is acceptable.

In Figure 22 the numerically obtained failure loads of bonded anchors, related to the average concrete cone failure load of headed anchors (Eqn. 1) with the same embedment depth are plotted as a function of the ratio embedment depth to bar diameter. In all cases failure was caused by concrete cone breakout. The figure shows, that the ratio of numerically-obtained failure loads in case of concrete cone failure ($N^0_{u,c,Bonded\ Anchor}$) to the calculated average failure load of headed anchors ($N^0_{u,c,Headed\ Anchor}$) decreases with increasing related embedment depth h_{ef}/d. This can be explained by the fact, that with a small ratio h_{ef}/d only one crack at the end of the anchor is formed (Fig. 19), while with a long embedment depth two or more internal cracks are formed (Fig. 20), which reduce the tensile capacity of the concrete in the region where failure occurs.

In Figure 23 the normalized failure loads yield by the analysis are plotted as a function of concrete compressive strength, the normalizing parameter being the failure load for $f_{cc} = 25$ N/mm². As with both cast-in-place headed anchors and post-installed mechanical anchors, increasing concrete compressive strength increases bonded anchors failure load, but not linearly, as shown by Equation 9:

$$\alpha_c = \left(\frac{f_{cc}}{25 N / mm^2} \right)^{0,5} \quad (-) \qquad (9)$$

This indicates that failure of bonded anchors is caused by concrete cone breakout.
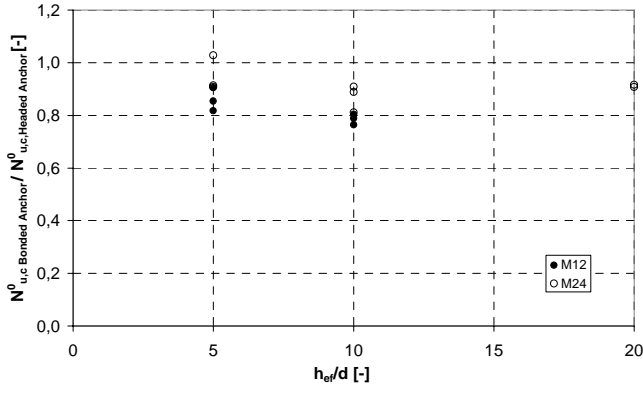
Figure 22. Ratio of numerically-obtained failure loads in case of concrete cone failure to the calculated average failure load of headed anchors as a function of the related embedment dept (h_{ef}/d).
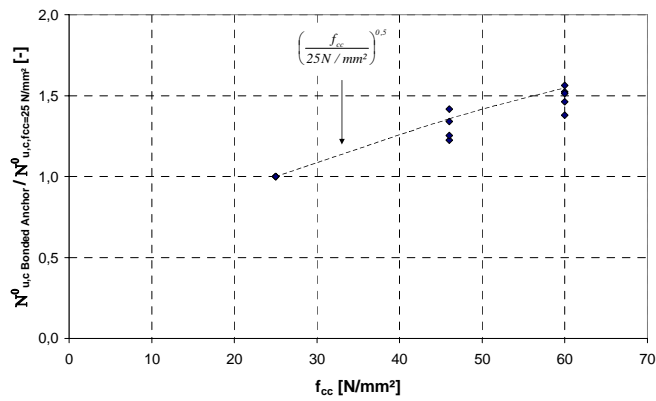

Figure 23. Ratio $N^0_{u,c,Bonded\ Anchor} / N^0_{u,c,fcc=25\ N/mm^2}$ as a function of the concrete compression strength.
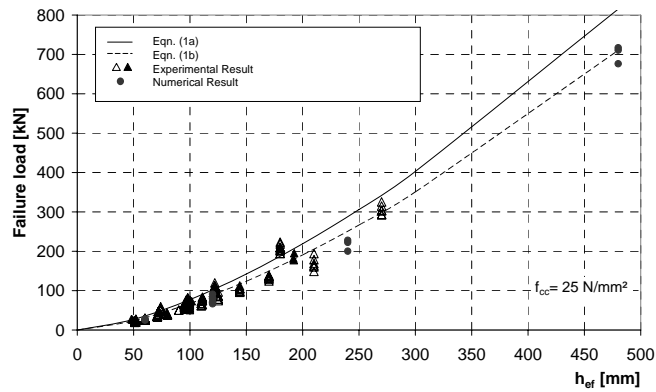

Figure 24. Numerically and experimentally obtained failure loads of bonded anchors in case of concrete cone failure as function of the embedment depth predicted according to Equation 1b.

Figure 24 shows the measured and numerically obtained failure loads of single bonded anchors normalized to $f_{cc} = 25$ N/mm² plotted as a function of the embedment depth. In the tests and the numerical analysis, failure was classified as concrete cone breakout. The failure loads increases in proportion to $h_{ef}^{1,5}$. On average they agree with concrete cone failure load of post-installed mechanical anchors.

Note that in case of pullout failure the failure load increases linearly with increasing embedment depth.

3.4.2 *Groups with bonded anchors*

Figure 25 shows principle tensile strains for a group of four adhesive anchors with $d = 12$mm, $h_{ef} = 5d$, and $\tau_u \geq \tau_{u,max}$ beyond the peak load. A single anchor with the same embedment depth would fail by a concrete cone failure. With a small spacing of $s = 4d$, the usual concrete breakout cone starting at the base of the anchors is formed (Fig. 25a). With a larger spacing ($s = 10d$) the angle of the crack between the neighboring bonded anchors increase (Fig. 25c). For a large spacing ($s = 18d$), the individual anchors of the group fail in the same way as a single anchors.
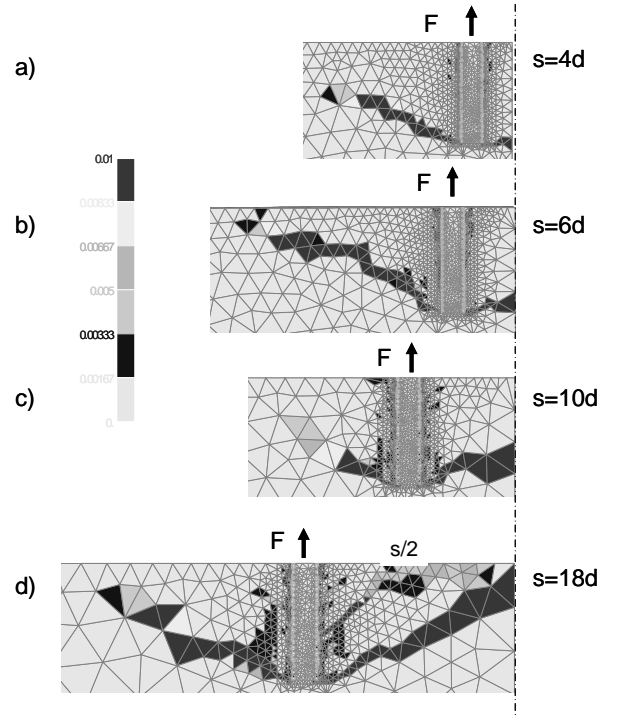

Figure 25. Concrete cone failure of quadruple anchor group predicted by numerical modeling for different spacing.

Figure 26 shows numerically-obtained failure loads of quadruple anchor groups with adhesive anchors for different values of the normalized embedment depth (s/h_{ef}).

As with cast-in-place headed and post - installed mechanical anchors the failure load of adhesive anchor groups increases with increasing spacing until it reaches a limit of *4* times the single anchor strength at a critical spacing $s_{cr,N}$. Similarly, the failure load of anchorages with adhesive anchors located near edges decreases when the edge distance is smaller than a critical value $c_{cr,N}$.

For each individual numerical test series, the critical spacing was evaluated from the results of the numerical analysis. The characteristic spacing related to the embedment depth is given as a function of the embedment depth related to *d* in Figure 27, where the characteristic spacing given in the CC–

Method ($s_{cr,N} = 3h_{ef}$) is plotted as well. For a small embedment depth the characteristic spacing is larger than $s_{cr,N} = 3h_{ef}$ while for larger embedment depth it approaches the value of $s_{cr,N} = 2h_{ef}$. This is due to the fact that the average slope of the cone for single bonded anchors with respect to the surface is increasing with increasing embedment depth (Fig. 19). This is generally confirmed by tests with groups of bonded anchors with $h_{ef} = 40$mm which failed by concrete cone breakout. The average failure load of the group at a spacing of $s = 3h_{ef}$ is only 2.5 times the failure load of a single anchor (Fig. 28). The results are more accurately predicted, when the characteristic spacing is assumed as $s_{cr,N} = 5h_{ef}$.

Figure 28. Measured failure loads of quadruple groups related to the measured failure load of a single anchor ($d = 12$, $h_{ef}/d = 4$, $\tau_u \sim \tau_{u,max}$).
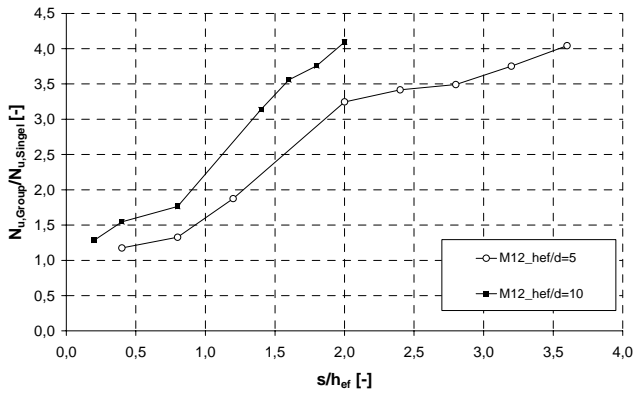

Figure 26. Numerically-obtained failure loads of quadruple groups related to the numerically failure load of a single anchor. Single anchors and anchor groups fail by a concrete cone failure.
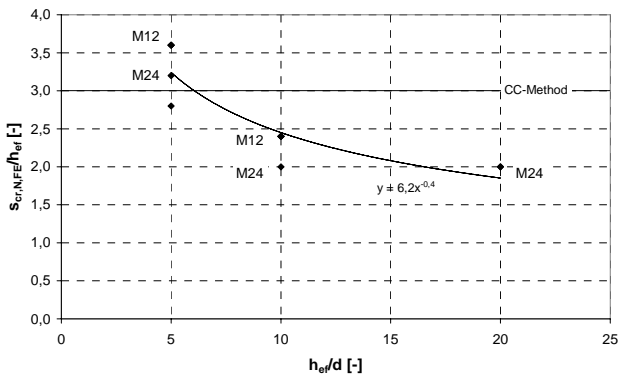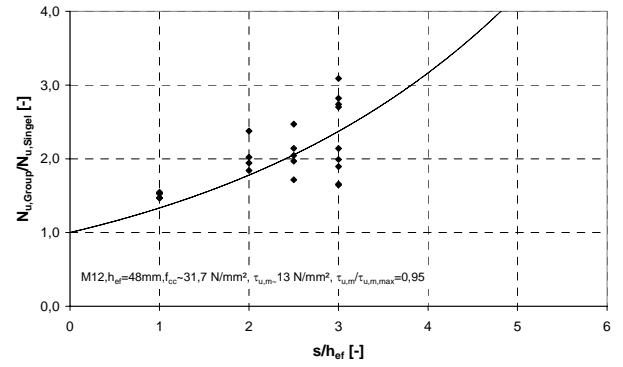

Figure 27. Numerically-obtained related characteristic spacing $s_{cr,N}/h_{ef}$ as a function of the related embedment depth (h_{ef}/d) in case of concrete cone failure.

In all numerical simulations, the calculated failure load of anchorages with adhesive anchors was smaller than the numerically obtained failure load of the same anchorages with headed anchors. Therefore, in Equation 2 and 8 the mean bond failure load, $N^0_{u,m,p}$ and $N_{u,m,p}$ is limited to the mean concrete breakout failure load, $N^0_{u,c}$ and $N_{u,c}$, given by Equation 1 and 2 for post-installed mechanical anchors.

4 BEHAVIORAL MODEL

The afore-mentioned numerical and experimental results made it possible to develop a behavioral model, that can accurately predict the failure loads of anchorages with adhesive anchors where the effects of anchor groups and/or edges needs to be accounted for. The proposed model can describe the two possible failure modes, either by concrete-cone breakout or by pullout failure. The behavioral model is represented by Equation 8 however, the characteristic spacing $s_{cr,Np}$ and characteristic edge distance $c_{cr,Np}$ provided by Equation 5 should be used when calculating $A_{p,N}$ and $A^0_{p,N}$ according to Figure 1, $\psi_{s,N}$ according to Equation 2b and $\psi_{g,N}$ according to Equation 7.

For design purposes, appropriate capacity-reduction factors and nominal strengths must be introduced in developing code provisions to implement the findings of this research. It is suggested that the 5% fractile of the bond strength be used for the design of bonded anchors which should be adjusted to consider several influencing factors on anchor performance such as sensitivity to hole cleaning procedures and increased temperature as well as long term behavior.

4.1 *Proposed Model versus available experimental results*

In Figures 29, 30, the ratios of the measured failure loads divided by the strengths predicted by the proposed model ($N_{u,test}/N_{u,calc}$) are plotted as a function of several parameters investigated in the tests. Figures 29 and 30 also show the "best fit" trend lines. If these lines are horizontal and are located at ($N_{u,test}/N_{u,calc}$) = 1.0 then the influence of the varied parameter on the failure load is well taken into account by the behavioral model. As indicated by these Figures the behavioral model provides an excellent fitting of the experimental results with groups. For the 415 tests the mean value of

$(N_{u,test}/N_{u,calc})$ is 0.99 with a coefficient of variation of 15.4%. An equally good prediction is obtained when the tests are divided into two groups, depending on whether anchor failure is due to concrete-cone failure or pullout failure (Tables 1). Summing up, the proposed behavior model for groups with adhesive anchors is as accurate as the behavior model for headed anchors. However, as shown in Figure 30 the predicted failure loads are conservative for anchorages located very close to a free edge.

The proposed model for adhesive anchors (Eqn. 8) is very similar to the behavioral model for headed anchors (Eqn. 2) except for the $\psi_{g,N}$ - factor in Equation 7.

Table 1 Comparison of measured failure loads with predicted values.

Type		Pullout and concrete breakout failure		
		n [-]	$\bar{x}$ [-]	v [%]
Group Tests	$N_{u,test}/N_{u,calc}$	415	0.99	15.4
Edge tests	$N_{u,test}/N_{u,calc}$	133	1.3	19.6

Type		Pullout failure		
		n [-]	$\bar{x}$ [-]	v [%]
Group Tests	$N_{u,test}/N_{u,calc}$	377	0.98	15.1
Edge tests	$N_{u,test}/N_{u,calc}$	133	1.3	19.6

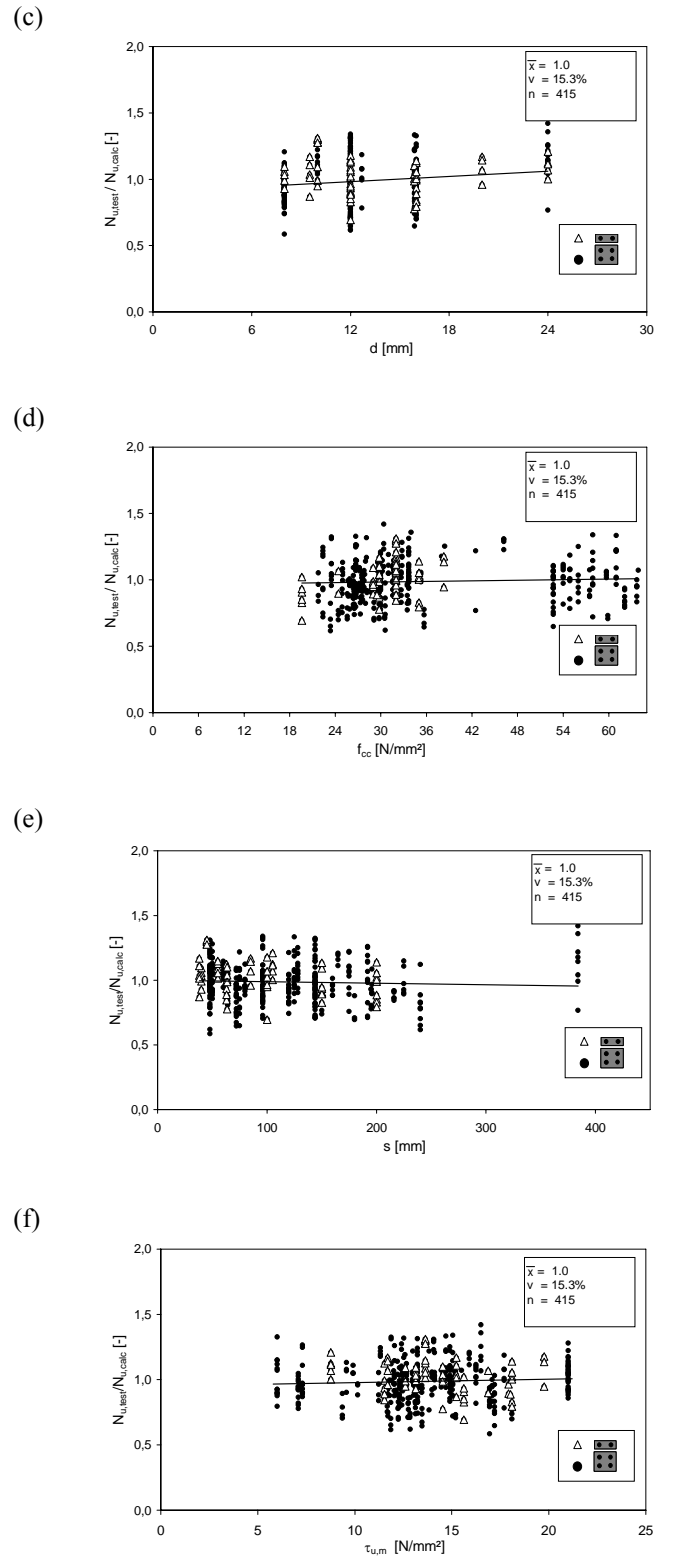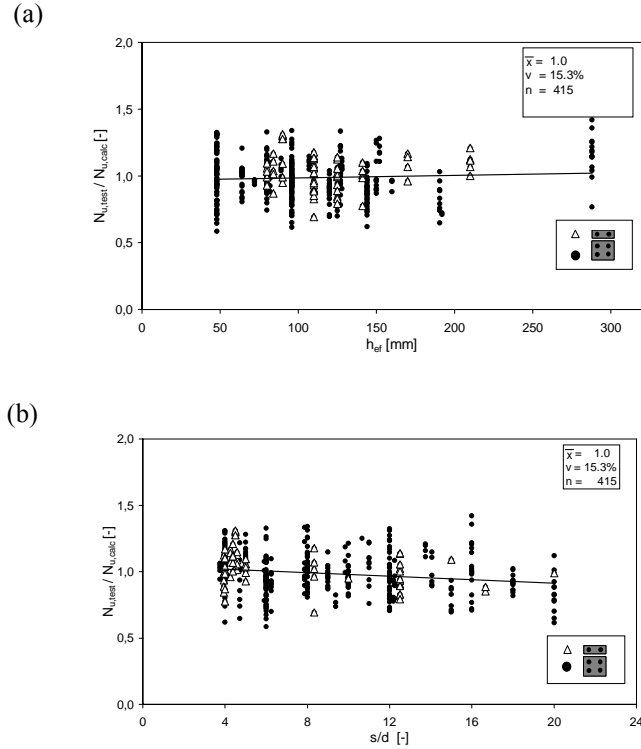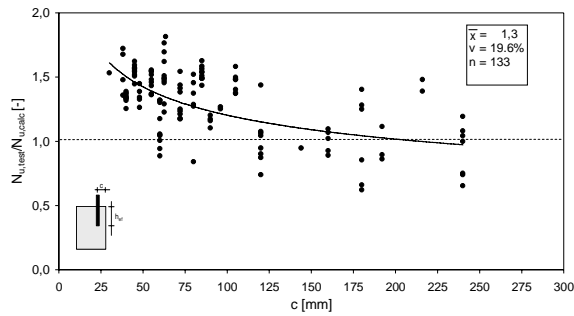| Type		Concrete breakout failure		
		n [-]	$\bar{x}$ [-]	v [%]
Group Tests	$N_{u,test}/N_{u,calc}$	38	1.05	16.3
Edge tests	$N_{u,test}/N_{u,calc}$	-	-	-

(a)

(b)

(c)

(d)

(e)

(f)

Figure 29. Proposed Model for anchor groups: fitting of tests results concerning: (a) effective embedment depth h_{ef}; (b) normalized anchors spacing s/d; (c) anchor diameter d; (d) concrete compressive strength f_{cc}; (e) anchor spacing s; and (f) average bond strength $\tau_{u,m}$.
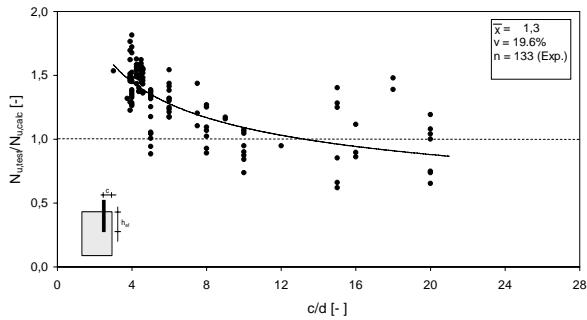
(a)

(b)

Figure 30. Failure loads of single anchors placed near a free edge: fitting of the tests results with the proposal mode, as a function of the edge distance c (a), and (b) of the normalized distance c/d.

5 SUMMARY AND CONCLUSIONS

Based on the results of both numerical and experimental investigations, a behavioral model to predict the average failure load of fastenings using adhesive bonded anchors is proposed. The model is similar to the behavioral model that predicts the concrete breakout failure load of cast-in-place and post-installed mechanical anchors but with the following modifications.

The basic strength of a single adhesive anchor predicts the pullout capacity and not the concrete breakout capacity. It is based on the uniform bond stress model as given by Equation 3. The characteristic spacing and characteristic edge distance of adhesive anchorages depend on the anchor diameter and the bond strength and not on the anchor embedment depth. Furthermore, an additional factor, $\psi_{g,N}$ is used, that takes into account the larger bond area of closely spaced adhesive anchors in comparison to a single anchor. The failure load of anchorages with adhesive anchors is limited to the concrete cone failure load of post-installed mechanical anchors.

The proposed behavioral model agrees very well with the results of 415 group tests contained in a worldwide data base. Based on a comparison to 133 tests with single anchors very near to an edge, the behavioral model is conservative for anchorages located very close to an edge.

REFERENCES

Appl, J. & Eligehausen, R. 2003. Gruppenbefestigungen mit Verbunddübeln – Bemessungskonzept- Groups of Bonded Anchors -Design Concept-), *Report* No. 03/27-2/55, Institute of Construction Materials, University of Stuttgart. Stuttgart

Cook, R.A., Kunz, J., Fuchs, W. & Konz, R.C. 1998. Behavior and Design of single Adhesive Anchors under Tensile Load in Uncracked concrete, *ACI Structural Journal,* V.95: pp 9-62

Eligehausen R., Mallée, R. & Silva J.F. 2006. *Anchorages in Concrete Construction.* Berlin: Ernst & Sohn

Eligehausen R., Appl, J., Lehr, B., Meszaros, J. & Fuchs, W. 2004. Tragverhalten und Bemessung von Verbunddübeln unter Zugbeanspruchung, Teil 1: Einzeldübel mit großem Achs- und Randabstand (Load bearing behavior of bonded anchors under tension loading, Part 1: Single bonded anchors far away from edges), *Beton- und Stahlbetonbau 99,* No. 7: pp. 561-571, Berlin: Ernst & Sohn

Fuchs, W., Eligehausen, R. & Breen, J.E. 1995. Concrete Capacity Design (CCD) Approach for Fastenings to Concrete, *ACI Structural Journal,* V.92, pp. 365-379

Li, Y.-J., Eligehausen, R., Ozbolt, J. & Lehr, B. 2002. Numerical Analysis of Quadruple Fastenings with bonded anchors, *ACI Structural Journal,* V.99, pp. 149-156

McVay, M., Cook, R.A. & Krishnamurthy, K. 1996. Pullout Simulation of Post-Installed Chemically Bonded Anchors, *Journal of Structural Engineering, ASCE,* V.122, pp1016-1024

Meszaros, J. 1999. Tragverhalten von Verbunddübeln in ungerissenem und gerissenem Beton (Load-Bearing behavior of bonded anchors in uncracked and cracked concrete). *Doctoral Thesis,* University of Stuttgart (in German)

Ozbolt, J. 1998. MASA-Finite Element Program for Nonlinear Analysis of Concrete and Reinforced Concrete Structures, *Research Report,* Institute of Construction Materials, University of Stuttgart